Critical Velocity of Continuous Vortex Nucleation in a Slab of Superfluid ^{3}He-A

P. M. Walmsley, D. J. Cousins, and A. I. Golov

Department of Physics and Astronomy, The University of Manchester, Manchester M13 9PL, United Kingdom

(Received 31 July 2003; published 24 November 2003)

A flow-induced Fréedericksz transition is observed in a 0.26 mm thick disk-shaped slab of superfluid ^{3}He-A using a rotating cryostat and a torsional oscillator, and it is used to detect vortices in zero magnetic field. The phenomena are studied as a function of magnetic field normal to the slab. In defect-free $\hat{\mathbf{l}}$ texture the critical velocity for vortex nucleation is 0.5 mm/s, but in the presence of a domain wall it is reduced to $\sim\hbar/2ma_c$, where $a_c(H)$ is the field-dependent radius of the vortex soft core. The vortices nucleate at a distance at least 0.3 mm from the outer edge of the disk.

DOI: 10.1103/PhysRevLett.91.225301 PACS numbers: 67.57.Fg, 47.32.–y, 64.60.Qb, 67.57.De

Phase slips, caused by moving zeros of the order parameter in singular cores of quantized vortex lines, are the standard mechanism of superflow decay in conventional superfluids and superconductors. ^{3}He-A is different as there is another mechanism dissipating the energy of flow by rotating its anisotropy axis $\hat{\mathbf{l}}$ without suppressing the order parameter [1]. Albeit very different microscopically, this process can still be described macroscopically as the nucleation and motion of *continuous* quantized vortices. Moreover, because in ^{3}He-A the relevant reorientations occur only on length scales greater than some 10 μm (much larger in small magnetic field) from container walls [2], the uncontrollable disorder due to the wall roughness does not make the vortex nucleation extrinsic as is the case in superfluid ^{4}He, ^{3}He-B, and superconductors. Hence, ^{3}He-A is the best available system in which to study the intrinsic nucleation of vortices as a hydrodynamic instability of flow in a well-controlled geometry. It also benefits from the existence of the microscopic theory for all hydrodynamic parameters.

Magnetic field H or container walls restrain the $\hat{\mathbf{l}}$ texture, hence stabilizing a finite value of the critical velocity of vortex nucleation, v_c. In this context, the question whether ^{3}He-A can sustain a finite nondissipative flow at $H = 0$ in a wide channel is in fact the test of *superfluidity* of ^{3}He-A. The interaction between $\hat{\mathbf{l}}$ and flow or other fields is hence a fundamental problem. These interactions also lead to the possibility of creating different metastable textures. Earlier attempts to measure v_c at $H = 0$ with a piston-driven flow [3] through a mm-sized rectangular channel revealed a broad range of $v_c =$ 0.5–2 mm/s, probably caused by poor control of textures. Continuous rotation is the only way to achieve steady flow in ^{3}He: this was recently employed in NMR studies of ^{3}He-A in a long rotating cylinder [2], but only in high magnetic field, $H =$ 100–300 G, and without full control of textures. They showed that the value of $v_c =$ 0.2–1.5 mm/s depends on the initial $\hat{\mathbf{l}}$ texture, and the presence of domain walls greatly reduces v_c.

We report reproducible measurements of critical velocities for flow-induced reversible and irreversible textural transitions in rotating ^{3}He-A. We gain control of the texture by placing ^{3}He-A in a slab of thickness D. This also imposes a length scale D which is the radius of the soft core of continuous vortices in zero field. We then apply magnetic field to control the vortex soft core size and to introduce a pair of domain walls on demand. We also describe a new vortex detection technique that is based on the sensitivity of a torsional oscillator to reorientation of $\hat{\mathbf{l}}$ caused by the counterflow surrounding the vortex cluster and can be used in zero field.

^{3}He-A is a fermionic superfluid [4] with the Cooper pairs in the p-wave spin-triplet state all having their orbital momentum locally pointing in the same direction $\hat{\mathbf{l}}(\mathbf{r})$. The spin anisotropy axis $\hat{\mathbf{d}}(\mathbf{r})$ tends to be aligned with $\hat{\mathbf{l}}$ because of the dipole-dipole interaction energy $F_d = -\frac{1}{2}\lambda_d(\hat{\mathbf{d}}\cdot\hat{\mathbf{l}})^2$. In what follows we consider this "dipole-locked" case $\hat{\mathbf{d}} = \pm\hat{\mathbf{l}}$ and call the spatial variation of $\hat{\mathbf{l}}(\mathbf{r})$ the *texture*.

Three competing effects orient the texture in a slab. First, the boundaries force $\hat{\mathbf{l}}$ normal to them favoring a uniform *normal texture* (NT) because tipping the $\hat{\mathbf{l}}$ vector in the middle of the slab costs kinetic energy $F_{slab} \sim K_b' D^{-2}$. Second, the magnetic energy in a perpendicular field $F_H = \frac{1}{2}\Delta\chi(\hat{\mathbf{d}}\cdot\mathbf{H})^2$ favors a uniform *planar texture* (PT) parallel to the walls; NT holds until the field [5]

$$H_F = (K_b'/\Delta\chi)^{1/2}(\pi/D), \tag{1}$$

above which $\hat{\mathbf{l}}$ bends over in a Fréedericksz transition [6]. Third, a counterflow $\mathbf{v} \equiv \mathbf{v}_n - \mathbf{v}_s$ parallel to the walls favors $\hat{\mathbf{l}}$ aligned with $\mathbf{v}$ due to the flow energy $F_v = -\frac{1}{2}\rho_0(\hat{\mathbf{l}}\cdot\mathbf{v})^2$, and hence should also cause a similar Fréedericksz transition from NT towards a uniformly tipped texture above the critical velocity [5,7]

$$v_F = (\rho_s^{\parallel}K_b'/\rho_s\rho_0)^{1/2}(\pi/D). \tag{2}$$

The critical velocity in magnetic field $v(H)$ [or critical field in the presence of flow $H(v)$] is predicted to satisfy [5]

$$(H/H_F)^2 + (v/v_F)^2 = 1. \tag{3}$$

 0031-9007/03/91(22)/225301(4)$20.00

The relative importance of various terms is as follows: the dipole locking F_d dominates the effect of confining walls F_{slab} at distances $D \gg \xi_d = (2K_b/\lambda_d)^{1/2} \approx 10\ \mu$m; F_d dominates the magnetic energy F_H in field $H \ll H_d = (\lambda_d/\Delta\chi)^{1/2} \approx 20$ G; F_H dominates F_{slab} at distances $D \gg \xi_H(H) = (2K_b/\Delta\chi)^{1/2}H^{-1} = \xi_d(H_d/H)$; the anisotropy of the flow energy F_v dominates the dipole locking F_d for velocities $v \gg v_d$,

$$v_d = (\lambda_d/\rho_0)^{1/2} = \hbar/2m\xi_d \approx 1 \text{ mm/s}. \quad (4)$$

Additionally, a term $F_l = -\frac{1}{2}\mathbf{v}\cdot C_0\hat{\mathbf{l}}[\hat{\mathbf{l}}\cdot(\nabla\times\hat{\mathbf{l}})]$ in the interaction between the counterflow and orbital currents favors helical winding of $\hat{\mathbf{l}}$ around $\mathbf{v}$. Hence, at a second higher critical velocity the aligned texture becomes unstable, typically leading to the creation of discrete continuous vortices, stable nonuniform $\hat{\mathbf{l}}$ textures with associated circulating v_s but without singularity of the order parameter in the core. The continuous vortices in a slab at $H = 0$ are of the two-quantum Anderson-Toulouse–type [1,8]. The vorticity is localized within their soft core of radius a_c, outside which the texture is uniform and the circulation of $\mathbf{v}_s$ is equal to $2\kappa_0$ [9]. For $H = 0$, $a_c \sim D$ while, for $H \gg H_d$, $a_c \sim \xi_d$. For H between $(\xi_d/D)H_d \sim H_F$ and H_d, it interpolates as $a_c(H) \sim \xi_H$.

In superfluid ^{4}He and ^{3}He-B superflow is topologically stable due to the quantization of the circulation. Dissipation in the form of discrete phase slips is prohibited by the macroscopic potential barrier to the nucleation of a vortex of critical size of order of the vortex core, after which the process of vortex growth is irreversible. The corresponding v_c is inversely proportional to the vortex core size [10]. These ideas successfully explained the observed values in ^{4}He and ^{3}He-B, and even in ^{3}He-A in high magnetic field [2,10]. ^{3}He-A is different as the circulation is not quantized and hence the superflow is not topologically stable at $H = 0$: rotation of $\hat{\mathbf{l}}$ (for example, in the form of moving continuous vortices) can dissipate kinetic energy continuously. Therefore in an open geometry and in zero field one would expect no potential barrier preventing such textural motion. In a slab the critical velocity would be inversely proportional to the soft core radius $a_c(D, H)$ [1,10],

$$v_a(D, H) \sim \hbar/2ma_c, \quad (5)$$

for $H = 0$, $v_a \sim \hbar/2mD \sim v_F$;
for $H_F \ll H \ll H_d$, $v_a \sim v_d(H/H_d)$;
for $H \gg H_d$, $v_a \sim \hbar/2m\xi_d = v_d$.

Thus, only in narrow channels or high fields one would have substantial $v_c \sim 1$ mm/s. However, because of the term F_v, coupling $\hat{\mathbf{l}}$ and $\mathbf{v}$, the $\hat{\mathbf{l}}$ texture aligned along $\mathbf{v}$ was predicted to be stable provided the texture is dipole locked [11]. Hence, aligned textures cannot nucleate vortices until the counterflow exceeds the dipole-unlocking critical velocity $\sim v_d$. The two models for v_c, Eqs. (4) and (5), predict similar values in fields $H > H_d$ but disagree considerably in the limit of $H = 0$ for $D \gg \xi_d$. To clarify the issue, we measured v_c at $H = 0$.

We studied liquid ^{3}He-A at pressure 29.3 bars in a disk-shaped volume of thickness $D = 0.26$ mm and radius $R = 5.0$ mm inside an epoxy torsional head on a BeCu stem. The disk's axis was aligned with that of the cryostat which could rotate continuously at angular velocity $\Omega =$ 0–1 rad/s while keeping the sample at the temperature of interest $T =$ 2–2.5 mK. The magnetic field $H =$ 0–25 G perpendicular to the disk was provided by a superconducting coil. The oscillator was driven capacitively at a frequency near its resonance, and the drive amplitude was kept sufficiently small so as not to affect the texture (large amplitude drive does persuade $\hat{\mathbf{l}}$ to align azimuthally with the ac flow [6]). The resonant frequency, $\nu_R \approx$ 627 Hz, and bandwidth ≈ 0.12 Hz of the torsional resonance were monitored as a function of T, Ω, and H. The viscous penetration depth was comparable with D for all orientations of $\hat{\mathbf{l}}$. As a result, ν_R is primarily sensitive to the temperature-dependent normal density $\rho_n(T)$ [which was used as an internal thermometer based on known $\rho_n(T)$ [6]] and reorientation of $\hat{\mathbf{l}}$ through the anisotropy of ρ_n. High-quality textures of ^{3}He-A were obtained by slowly cooling (at rate $\sim 1\ \mu$K/ min) through T_c at $H = 0$ while rotating at $\Omega = 0.46$ rad/s; NT was produced after rotation was stopped below T_c.

While rotating at Ω (and with N two-quantum vortices forming a vortex cluster) the counterflow at radius r outside the vortex cluster is

$$v(N, \Omega, r) \equiv v_n(\Omega, r) - v_s(N, r) = \Omega r - 2\kappa_0 N/2\pi r. \quad (6)$$

$v(r)$ is highest near the outer edge at $r \approx R$, because $R \gg D$ the flow there is approximately straight and uniform; hence, the Fréedericksz transition should first occur at $r \approx R$ when $v(R) = v_F$. However, the boundary conditions at the outer edge additionally stiffen the texture within some $\sim D$ from the edge. Hence, we assume that the transition starts at some radius $R_F \approx R$ ($R - R_F \sim D$) and then propagates inwards at radius $r_F(\Omega)$ such that $v(r_F) = v_F$. Between $r_F(\Omega)$ and R_F, $\hat{\mathbf{l}}$ tends to be aligned with $\mathbf{v}$ to form *azimuthal texture* (AT).

The Fréedericksz transition was detected by the shift in $\nu_R(\Omega)$ caused by the reorientation of $\hat{\mathbf{l}}$ as in the studies of the field-induced Fréedericksz transition [6,12]. An example is shown in Fig. 1. The frequency shift above Ω_F is sharp and reversible. Between three and eight vortices ($N_0 =$ 3–8) always remained weakly pinned in the slab after sufficiently fast rotation, presumably, by irregularities of the slab surfaces. Their circulation, $2\kappa_0 N_0$, biased the apparent values of Ω_F (open circles in Fig. 2) by $\Omega_0 = 2\kappa_0 N_0/2\pi R^2 =$ 0.003–0.007 rad/s. These vortices could be removed by slow rotation to $\Omega =$ -0.01 rad/s in the opposite direction, after which the

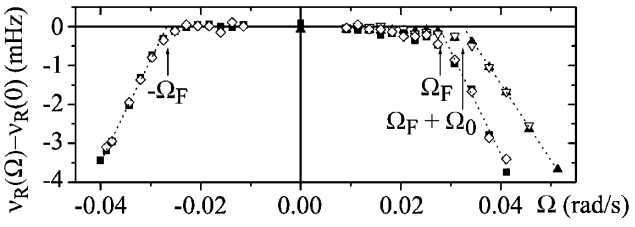

FIG. 1. Frequency shift vs angular velocity in a sample with trapped vortices (triangles) and after removing them (squares, diamonds), during acceleration (closed symbols) and deceleration (open symbols). The onsets of the Fréedericksz transitions are labeled; dashed lines guide the eye. $T = 0.92T_c$.

bias disappeared, and the vortex-free texture was stable for rotation with $\Omega < v_c/R$ (Fig. 1). The value of Ω_F was then the same for rotation in both directions (closed circles in Fig. 2). It increases slightly with temperature; the equivalent linear velocity $\Omega_F R$ (right axis in Fig. 2) extrapolates to 0.16 mm/s at T_c which is close to $v_F = 0.14$ mm/s as predicted by Eq. (2) for homogeneous flow in an infinite slab. At all temperatures, $\Omega_F R$ is slightly higher than the values of v_F calculated from Eq. (2). The apparent disagreement can be completely resolved if we set $R_F = 4.65$ mm.

The measured ν_R during a typical rotation sweep from $\Omega = 0$ to $\Omega_{max} = 0.46$ rad/s at $H = 0$ and $T = 0.95T_c$ is shown in Fig. 3 (the bandwidth shows the same features, but its signal-to-noise ratio is worse [13]). While accelerating, there are three regimes separated by angular velocities $\Omega_F = 0.03$ rad/s and $\Omega_c = 0.12$ rad/s. Only if Ω_{max} exceeded Ω_c do the values of $\nu_R(\Omega)$ on deceleration become different: it returns to the initial value $\nu_R(0)$ not at Ω_F but at $\Omega_{min} = 0.34$ rad/s (the value of Ω_{min} depends on Ω_{max}) and then stays constant all the way down to $\Omega = 0$. A number of sweeps up to different Ω_{max} have been performed at different temperatures and for different samples of defect-free textures. They were reproducible provided the rotation was always in the same

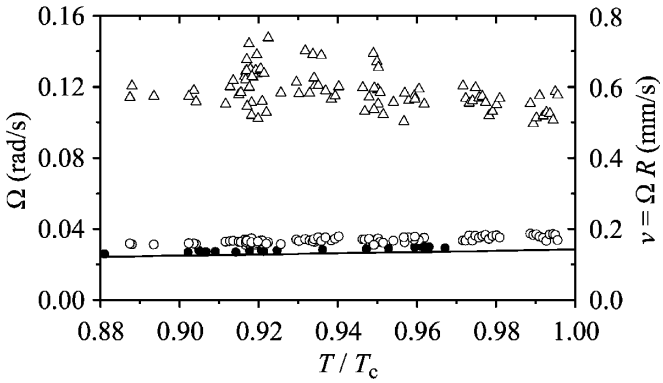

FIG. 2. Temperature dependence of the critical velocities Ω_F (circles) and Ω_c (triangles) and corresponding $\Omega_F R$, $\Omega_c R$ (right axes) at $H = 0$ in six samples. The line follows Eq. (2).

direction as that used during the initial cooling through T_c(rotation in the opposite direction produces static textural defects).

To model $\nu_R(\Omega)$ at $H = 0$, we assume that between $r_F(\Omega)$ and R_F the texture switches from NT to AT, the latter having higher normal density. This causes the increase in the moment of inertia $\Delta I(r_F) \propto (R_F^4 - r_F^4)$ and hence the frequency shift $\nu_R(\Omega) - \nu_R(0) = \Delta\nu_R(r_F^4(\Omega) - R_F^4)$, where $\Delta\nu_R(T)$ is a fitting parameter. Vortices nucleate at a critical distance from the edge (i.e., at a radius $R_c < R$) when $v(R_c)$ reaches v_c. There are three different states during acceleration [(a), (b), (c)] and two during deceleration [(d), (e)] (see the cartoons in Fig. 3). (a) $0 < \Omega < \Omega_F$: NT everywhere. (b) $\Omega_F < \Omega < \Omega_c$: The Fréedericksz transition propagates inwards at $r_F(\Omega)$ maintaining $v(N_0, \Omega, r_F) = v_F$. (c) $\Omega_c < \Omega$: Vortices nucleate and move to the center of the disk maintaining $v(N, \Omega, R_c) = v_c$. (d) $\Omega_{min} < \Omega < \Omega_{max}$: During deceleration from Ω_{max} to Ω_{min}, $N_{max} = \text{const}$, where $v(N_{max}, \Omega_{max}, R_c) = v_c$. (e) $\Omega < \Omega_{min}(\Omega_{max})$: When $v(N_{max}, \Omega_{min}, R_F) = v_F$, r_F reaches R_F again and the belt of tipped texture disappears; the vortices soon start to annihilate as Ω decreases, thus maintaining zero average counterflow.

The conditions (a)–(e) yield the relation

$$R_c^2(\Omega_{max} - \Omega_c) = R_F^2(\Omega_{min} - \Omega_F). \quad (7)$$

Hence there are four independent parameters in the model: $\Omega_F, \Omega_c, R_c/R_F, \Delta\nu_R$. The solid line in Fig. 3 is the fit to the experimental data. This yields the ratio of $R_c/R_F = 0.94 \pm 0.02$, the same as given by Eq. (7) using hand-picked values of $\Omega_F, \Omega_c, \Omega_{min}(\Omega_{max})$. We also show in Fig. 3 the best fit with fixed value of $R_c = R_F$, which is clearly inadequate. Thus, R_c is ≈ 0.3 mm smaller than

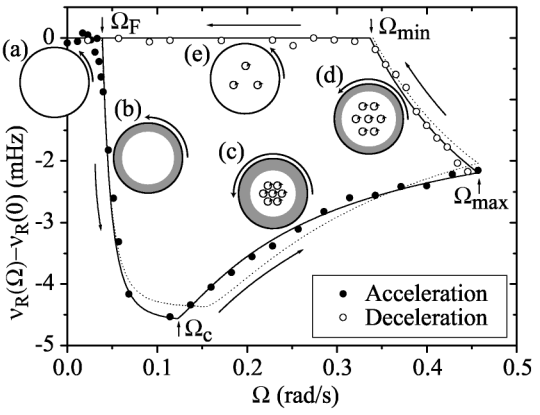

FIG. 3. Frequency shift during a rotation sweep to $\Omega_{max} = 0.46$ rad/s and back. The cartoons represent five different regimes separated by $\Omega_F, \Omega_c, \Omega_{max}, \Omega_{min}$ (white background, NT; grey, AT). Within our model, the shift in ν_R is proportional to the extra moment of inertia of the grey outer belt with the inner radius $r_F(\Omega)$. The solid (dotted) line is the fit with $R_c = 0.94R_F$ ($R_c = R_F$). $T = 0.95T_c$.

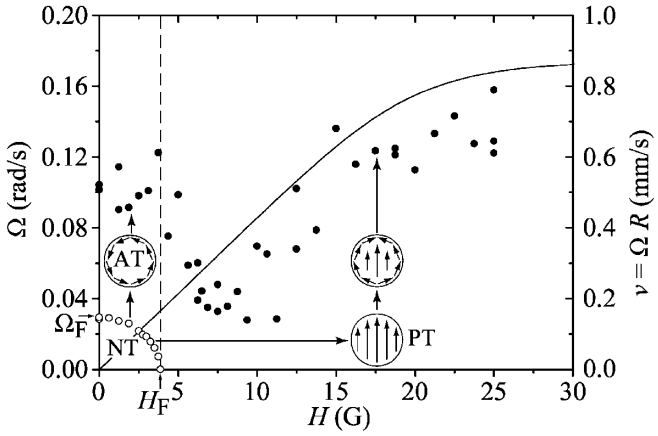

FIG. 4. Magnetic field dependence at $T = 0.90T_c$ of Ω_F and Ω_c (left axis), and $\Omega_F R$ and $\Omega_c R$ (right axis). The solid line is the theoretical threshold for the onset of dissipation at $T = 0.90T_c$ of a uniform flow through a domain wall from [14]. The vertical dashed line at $H = H_F$ indicates switching between two initial textures of different symmetries: the azimuthal flow (left cartoon) and two domain walls (right cartoon).

R_F, which itself should be within $\sim D$ from R. Assuming $R_F = 4.65$ mm takes R_c to $0.94R_F \approx 4.4$ mm. This agrees with the expectation that the vortices nucleate at a critical distance from the wall about the soft core size, which is $\sim D$ at $H = 0$.

The fitting parameter Ω_c is shown by triangles in Fig. 2 and also as equivalent linear velocities $\Omega_c R$. For each sweep the small bias Ω_0 (mean 0.005 ± 0.001 rad/s), due to trapped vortices, was subtracted. The value of Ω_c is fairly temperature independent and averages to $\Omega_c R = 0.59 \pm 0.05$ mm/s or, if $R_c = 4.4$ mm is used, to $\Omega_c R_c = 0.52 \pm 0.04$ mm/s. The scatter is modest suggesting that we achieved a good control of the initial texture. The values are consistent with the estimate $v_c \sim 1$ mm/s from Eq. (4) for the critical velocity for the texture stabilized by the parallel flow. On the other hand, the calculated threshold for the instability of the helical texture in a bulk flow at $H = 0$ near T_c [14] is $1.3v_d = 1.4$ mm/s. One possible explanation of the discrepancy is that our texture at R_c is not perfectly aligned with the flow because of the walls and outer edge; hence the stabilizing effect of the term F_v is reduced.

In magnetic field, the Fréedericksz transition (open circles in Fig. 4) was observed both by sweeping Ω while keeping H constant and by sweeping H while keeping Ω constant. The values of $v_F(H)$ follow Eq. (3).

The critical velocities $\Omega_c(H)$ and $v_c(H) = \Omega_c R$ (closed circles in Fig. 4) were obtained in rotation sweeps, $0 \rightarrow \Omega_{max} \rightarrow 0$, while keeping the field H constant; one can see a minimum of $\Omega_c(H) \approx \Omega_F(0) = 0.03$ rad/s at $H \approx$ 6–12 G. However, if we first set rotation at Ω such as $\Omega_F < \Omega < \Omega_c(0)$ and then swept H from 0 to 25 G and back, no vortices are nucleated. This indicates that one can have two topologically different $\hat{\mathbf{l}}$ textures in rotation (see the cartoons in Fig. 4): at $H < H_F$ it is a defect-free rotationally invariant AT [formed during initial acceleration at $H < H_F(0)$, and preserved even after subsequent sweeping H well above H_F]; while at $H > H_F$ the texture evolves from a PT into a state where the azimuthal counterflow crosses two domain walls (increased rotation only deforms it in the azimuthal direction, but preserves the mirror symmetry). The calculated critical velocity [14] for the dissipation onset in a bulk flow through a dipole-locked domain wall (line in Fig. 4) is in good agreement. This line actually follows quite closely the predictions of Eq. (5) for $H > H_F$.

Thus, provided there are no textural defects, ^{3}He-A can maintain a substantial steady nondissipative counterflow even in a 0.26 mm thick channel and a small magnetic field. The critical velocity $v_c \approx 0.5$ mm/s is set by dipole unlocking. Domain walls suppress it to $v_c \sim \hbar/2ma_c$.

We acknowledge regular discussions with H. Hall and the contribution of S. May in the design and construction of the experiment. Support provided by EPSRC under GR/N35113.

[1] P. W. Anderson and G. Toulouse, Phys. Rev. Lett. **38**, 508 (1977).
[2] V. M. H. Ruutu *et al.*, Phys. Rev. Lett. **79**, 5058 (1997).
[3] P. D. Saundry *et al.*, J. Low Temp. Phys. **86**, 401 (1992).
[4] D. Vollhardt and P. Wölfle, *The Superfluid Phases of Helium 3* (Taylor & Francis, London, 1990).
[5] A. L. Fetter, Phys. Rev. B **14**, 2801 (1976).
[6] J. R. Hook *et al.*, J. Low Temp. Phys. **74**, 45 (1989).
[7] C.-R. Hu, Phys. Rev. B **20**, 276 (1979).
[8] H. E. Hall and J. R. Hook, in *Progress in Low Temperature Physics*, edited by D. F. Brewer (Elsevier Science Publishers B.V., Amsterdam, 1986), Vol. IX.
[9] M. M. Salomaa and G. E. Volovik, Rev. Mod. Phys. **59**, 533 (1987).
[10] G. E. Volovik, V. B. Eltsov, and M. Krusius, in *Vortices in Unconventional Superconductors and Superfluids*, edited by R. P. Huebener, N. Schopohl, and G. E. Volovik (Springer, Berlin, 2002).
[11] P. Bhattacharyya, T.-L. Ho, and N. D. Mermin, Phys. Rev. Lett. **39**, 1290 (1977).
[12] P. M. Walmsley, D. J. Cousins, H. E. Hall, and A. I. Golov, Physica (Amsterdam) **329B–333B**, 68 (2003).
[13] P. M. Walmsley, D. J. Cousins, and A. I. Golov, J. Low Temp. Phys. (to be published).
[14] J. Kopu, R. Hänninen, and E. V. Thuneberg, Phys. Rev. B **62**, 12374 (2000).